Published in final edited form as:

Oncogene. 2011 March 24; 30(12): 1449–1459. doi:10.1038/onc.2010.526.

MUC1 enhances invasiveness of pancreatic cancer cells by inducing epithelial to mesenchymal transition

Lopamudra Das Roy[1], **Mahnaz Sahraei**[1], **Durai B. Subramani**[2], **Dahlia Besmer**[1], **Sritama Nath**[1], **Teresa L. Tinder**[2], **Ekta Bajaj**[2], **Kandavel Shanmugam**[2], **Yong Yook Lee**[3], **Sun IL Hwang**[3], **Sandra J. Gendler**[2], and **Pinku Mukherjee**[1,*]

[1]University of North Carolina at Charlotte, Department of Biology, Charlotte, NC-28223

[2]Mayo Clinic School of Medicine in Arizona, Department of Biochemistry and Molecular Biology, Scottsdale, AZ-85259

[3]Carolinas Healthcare Center, Charlotte, NC-28204

Abstract

Increased motility and invasiveness of pancreatic cancer cells are associated with epithelial to mesenchymal transition (EMT). Snai1 and Slug are zinc-finger transcription factors that trigger this process by repressing E-cadherin and enhancing vimentin and N-Cadherin protein expression. However, the mechanisms that regulate this activation in pancreatic tumors remain elusive. MUC1, a transmembrane mucin glycoprotein, is associated with the most invasive forms of pancreatic adenocarcinomas (PDA). In this study, we show that over expression of MUC1 in pancreatic cancer cells triggers the molecular process of EMT which translates to increased invasiveness and metastasis. EMT was significantly reduced when Muc1 was genetically deleted in a mouse model of PDA or when all seven tyrosines in the cytoplasmic tail of MUC1 were mutated to phenylalanine (mutated MUC1 CT). Using proteomics, RT-PCR, and Western blotting, we revealed a significant increase in vimentin, Slug and Snail expression with repression of E-Cadherin in MUC1-expressing cells compared to cells expressing the mutated MUC1 CT. In the cells that carried the mutated MUC1 CT, MUC1 failed to co-immunoprecipitate with β-catenin and translocate to the nucleus thereby blocking transcription of the genes associated with EMT and metastasis. Thus, functional tyrosines are critical in stimulating the interactions between MUC1 and β-catenin and their nuclear translocation to initiate the process of EMT. This study signifies the oncogenic role of MUC1 CT and is the first to identify a direct role of the MUC1 in initiating EMT during pancreatic cancer. The data may have implications in future design of MUC1-targeted therapies for pancreatic cancer.

Corresponding Author Previous address: Pinku Mukherjee, Ph.D., Associate Professor, Department of Immunology, Director, Cellular Immunology Laboratory, Mayo Clinic Arizona, 13400 E. Shea Blvd., Scottsdale, AZ 85255, Phone: 480-301-5168, Fax: 480-301-7017, mukherjee.pinku@mayo.edu.
Present address: Irwin Belk Endowed Professor of Cancer Research, Department of Biology, University of North Carolina Charlotte, 9201 University City Blvd., Charlotte, NC 28223, Phone: 704-687-5459, Fax: 704-687-3128, pmukherj@uncc.edu

Conflict of Interest:
Drs. Mukherjee and Gendler work has been funded by the NIH. There are no other conflicts to declare. All other authors declare no conflicts of interests.

Introduction

Pancreatic Ductal Adenocarcinoma (PDA) is the fourth leading cause of cancer-related death in the United States (1). This disease remains a major therapeutic challenge, as it is naturally resistant to current chemotherapy/radiation treatments. Poor prognosis has been attributed to delayed diagnosis, early vascular dissemination, and metastases to distant organs, especially the liver and peritoneum (2). One important insight came from the discovery that the increased motility and invasiveness of cancer cells are associated with epithelial to mesenchymal transition (EMT) (3–4). In EMT, epithelial cells acquire fibroblast-like properties and show reduced intercellular adhesion and increased motility. This process is associated with the transcriptional repression and functional loss of E-cadherin (3–4). Several transcription factors have been implicated in this repression, including the zinc-finger proteins of the Snail/Slug family (5–7), δEF1/ZEB1, SIP1 (8), and the basic helix-loop-helix E12/E47 factor (9). Snail was shown to repress the expression of E-cadherin and induce EMT in several cancer cells (5–7). Although several factors such as TGF-β and the estrogen receptor were shown to regulate Snail transcription (10–11), the mechanisms that modulate the function of Snail have remained largely elusive. Recently, dual regulation of Snail by GSK-3β-mediated phosphorylation has been implicated in EMT (12).

MUC1 is a transmembrane mucin glycoprotein that is over-expressed and aberrantly glycosylated in >90% of metastatic PDA (13). Although elevated levels of MUC1 protein have been associated with higher metastasis and poor prognosis, its molecular role in metastasis remains unclear (14–17). Multiple reports have appeared over the past decade demonstrating an incredible range of intracellular signaling functions associated with the 72–amino acid residue of the MUC1 cytoplasmic tail (MUC1 CT) which is reviewed in (18–20). MUC1 CT is a target for several kinases, including ζ̃chain–associated protein kinase of 70 kD (ZAP-70), the δ isoform of protein kinase C (PKCδ), glycogen synthase kinase 3̣ (GSK-3β), and the tyrosine kinases c-Src and Lck (21–23). Phosphorylation of the tyrosine within the TDRSPYEKV sequence by c-Src and Lck stimulates interactions between MUC1 and β-catenin whereas phosphorylation of Ser by GsK-3β inhibits this interaction (24–25). The same tyrosine residue is critically important for nuclear localization of MUC1, apparently because of the requirement for tyrosine phosphorylation to support the appropriate interactions necessary for intracellular trafficking. Binding to β-catenin appears to provide the signals required for movement of MUC1 to the nucleus in tumor cells (18) thereby influencing transcription through TCF/LEF and/or other transcription factors (20).

We have generated human pancreatic cancer cell lines that express wildtype MUC1 or mutated MUC1 CT in which all 7 tyrosines are mutated to phenylalanine. We have also generated mouse models of PDA that either expresses human MUC1 (17) or genetically lack Muc1. Cell lines have been developed from these mice to study the oncogenic role of MUC1 in pancreatic cancer progression. In this study, we show that EMT and secondary metastasis was significantly reduced in PDA mice that lack Muc1 compared to PDA mice that express MUC1. In contrast, over expression of MUC1 in both human and mouse pancreatic cancer cells initiated EMT by inducing the transcription factors Snail and Slug and repressing E-Cadherin, which lead to increased invasion and metastasis. Furthermore, mutating the

tyrosines in MUC1 CT to phenylalanine completely blocked EMT and prevented metastasis. The data suggests direct oncogenic signaling through the tyrosines of MUC1 CT in the induction of EMT and metastasis during pancreatic cancer.

RESULTS

Lower incidence of metastasis in PDA.Muc1KO mice compared to PDA.MUC1 mice: Evidence of EMT in PDA.MUC1 tumors

PDA.MUC1 and PDA.Muc1KO mice were sacrificed at ~36–40 weeks of age when all mice had primary pancreatic tumors. When organs were evaluated for macroscopic lesions, sixty percent (8/13 mice) of the PDA.MUC1 mice developed lung metastasis with ~40% (5/13) developing liver and ~20% (3/13) developing peritoneum metastasis (Figure 1B). This was in contrast to PDA.Muc1KO mice where only 1 out of 10 mice developed metastasis in all three organs. To investigate the mechanism by which MUC1 initiated higher metastasis, we evaluated if MUC1 plays a role in activating the EMT-associated proteins in the primary tumors. Tumor lysates from PDA.MUC1 and PDA.Muc1KO tumors (n=5) were analyzed by proteomics. Several proteins were differentially expressed; however, the most notable differences were in the levels of Vimentin and E-Cadherin. In the PDA.MUC1 tumors, there was a significant 5-fold increase in Vimentin with a concurrent decrease in E-Cadherin (Figure 1C and D). In contrast, the pattern was completely reversed in the PDA.Muc1KO tumors with significantly higher (4-fold) levels of E-Cadherin and lower levels of Vimentin (Figure 1D and C). The data was the first indication of possible induction of EMT in the MUC1-expressing tumors. Repression of E-Cadherin and induction of Vimentin in the PDA.MUC1 tumors directly correlated with increased metastasis in the PDA.MUC1 mice.

MUC1 promotes induction of mesenchymal markers and functionally enhances the invasive capacity of pancreatic cancer cells *in vitro*

To further confirm the role of MUC1 in EMT, KCKO and KCM cell lines were generated from the PDA.Muc1KO and PDA.MUC1 mice respectively. MUC1 expression was confirmed by Western blotting (Figure 1E) using MUC1 tandem repeat (TR, B27.29) and MUC1 CT (CT2) antibodies with high expression detected in KCM and no expression in KCKO cells (Figure 1E). B27.29 antibody detects the high molecular weight extracellular domain (>200 kD) and CT2 detects the low molecular weight CT domain (30kD). Both cell lines were subjected to an *in vitro* invasion assay, results of which showed significantly higher invasion index of the KCM compared to the KCKO cells ($p<0.01$, Figure1F), confirming MUC1 as the major contributor of increased motility and invasiveness. Furthermore, presence of MUC1 in KCM tumors clearly repressed E-Cadherin expression (Figure 1D) and induced expression of transcription factors and proteins associated with the mesenchymal phenotype. These included Snail, Slug, N-cadherin, and Vimentin (Figure 1G), which potentially contributed to the contact inhibition and high invasion *in vitro* and *in vivo* (Figure 1F and 1B). Lastly, KCM cells expressed higher levels of vascular endothelial growth factor (VEGF) compared to KCKO cells (Figure 1G), another indicator of highly metastatic phenotype. Thus, we hypothesized that MUC1 induces EMT and initiates invasion in mouse pancreatic cancer cells.

Over expression of MUC1 in human pancreatic cancer cells promotes EMT and induces invasion: Role of tyrosines in the MUC1 CT

To further test our hypothesis and delineate the potential mechanism, we stably infected human pancreatic cancer cell lines, BxPC3 and Su86.86 with full length MUC1 or mutated MUC1 CT. Cells expressing full length MUC1 were designated BxPC3.MUC1 and Su86.86.MUC1 while cells expressing mutant MUC1 CT were designated BxPC3.Y0 and Su86.86.Y0. Cells infected with an empty vector containing the neomycin resistance gene were used as controls and designated BxPC3.Neo and Su86.86.Neo. The only difference between MUC1 and Y0 constructs was that in Y0 construct, all 7 tyrosines in MUC1 CT were replaced by phenylalanine. Expression of MUC1 was confirmed in both cell lines by Western blotting (Figure 2A – D) using both the B27.29 and CT2 antibodies. The small shift in electrophoretic mobility noted in the Y0 cell lysate relative to MUC1 cells likely reflects a decrease in phosphorylation due to the mutations of the tyrosine residues in the Y0 cells (Figure 2B and D). An *in vitro* invasion assay showed significantly higher invasion index for MUC1 cells as compared to Y0 and Neo cells ($p<0.01$, Figure 2E and F). These data suggest that the increased invasiveness of the MUC1-expressing cells may be attributed to the tyrosines in the MUC1 CT. To substantiate the role of the MUC1 CT tyrosines as an inducer of EMT, real-time PCR arrays were used to explore transcription of 72 genes implicated in EMT and metastasis. Genes whose transcription was altered by at least 2-fold compared to Neo-cells were considered significant. Several genes associated with tight junctions and epithelial phenotype was significantly reduced in BxPC3-MUC1 compared to the Neo cells. These included Tight Junction Proteins 1 and 3, Occludin, Laminin α5, β-and δ-catenin, Claudin, and E-cadherin (Figure 2G). In contrast, there was no such change in the Y0 cells (Figure 2G). Conversely, genes associated with the mesenchymal phenotype and invasion was significantly increased in the BxPC3 MUC1 and decreased in the Y0 cells compared to Neo cells. These included Vimentin, Twist, Slug, Snail, and Goosecoid, (Figure 2H). Both functional and molecular studies indicate that MUC1 initiates the process of EMT via signaling through the tyrosines in its CT and that no external factor is necessary to stimulate these changes.

Loss of epithelial and gain of mesenchymal markers in MUC1 but not in Y0 cells directly corresponds to their transcription of metastasis-associated genes

At the protein level, gain of mesenchymal markers such as Slug, Snail and Vimentin and loss of E-cadherin expression was apparent in the MUC1 cells (Figure 3 A – D). These alterations in protein expression compared to Neo cells was not detected in the Y0 cells, implicating the importance of the tyrosines for effective oncogenic signaling and induction of EMT (Figure 3 A – D). Downregulation of E-cadherin was further confirmed by confocal microscopy in BXPC3 MUC1 but not in the Y0 cells (Figure 3E). It is well established that Snail represses the expression of E-cadherin to induce EMT in several cancer cells (5–7). Thus, data clearly suggests that MUC1 plays a critical role in inducing EMT in human pancreatic cancer cell lines via signaling through its CT tyrosines. Furthermore, genes associated with metastasis and angiogenesis such as VEGF, MMP-9, 3, & 2 and IL-6R were significantly increased in BxPC3 MUC1 but not in the Y0 cells compared to Neo controls

(Figure 3F). Therefore, we propose that without functional tyrosines in MUC1 CT, EMT and metastasis may be blocked in human pancreatic cancer cells.

Circulating tumor cells (CTCs) detected in mice bearing the BxPC3-MUC1 but not Neo or Y0 tumors

To test tumor growth and metastasis *in vivo*, BxPC3-MUC1, Y0 and Neo cells were subcutaneously injected into nude mice. All cells formed tumors within 15 days post injection with tumor growth being significantly higher in BxPC3 MUC1 versus Y0 and Neo tumors (Figure 4A (*p=0.02 – 0.05). BxPC3 MUC1 and Y0 tumors expressed high levels of MUC1 while Neo tumors expressed negligible amounts of MUC1 (Figure 4B). We were unable to detect gross metastatic lesions from these tumors; therefore we evaluated levels of CTCs in the blood of these mice. Within 2-weeks of culture, we were able to detect colonies of tumor cells in the blood collected from BxPC3-MUC1 but not from Neo or Y0 tumor-bearing mice (Figure 4C). The data signifies the role of MUC1 CT tyrosines during pancreatic cancer growth and extravasation of the cells into the blood stream for future metastasis.

Detection of EMT *in vivo* in BxPC3-MUC1 tumors

Protein lysates from the tumors were analyzed for the epithelial and mesenchymal markers. Similar to the *in vitro* data in Figure 3, the BxPC3 MUC1 tumor lysate showed downregulation of E-Cadherin (Figure 4D) and upregulation of Slug, Snail, and Vimentin (Figure 4E) clearly indicating the initiation of EMT *in vivo*. This process was completely abrogated when the tyrosines were mutated even though high levels of MUC1 protein was being expressed in the Y0 tumors (Figure 4B).

Significantly higher levels of pro-metastatic and pro-angiogenic growth factors in the BXPC3 MUC1 tumor microenvironment compared to Y0 or Neo tumors

To determine the effect of EMT on the tumor microenvironment itself, we tested the protein levels of some of the known mediators of metastasis and angiogenesis in the tumor lysates using the Ray Biotech protein array kit. Two-fold or more increase was considered significant and is represented (Figure 4F). Significant increases in levels of circulating VEGF (10-fold), insulin-like growth factor-1 (IGF-1, 2-fold), interleukin-6 (IL-6, 3-fold) and its receptor (IL-6R, 2.2-fold), stem cell factor (SCF, 2.5 fold), P-selectin (20-fold), and epidermal growth factor (EGF, 2.8-fold) were observed in the BxPC3 MUC1 tumors compared to the Neo and Y0 tumors. VEGF expression was also determined by IHC in the tumor sections with high levels detected in the BxPC3 MUC1 tumors versus Neo and Y0 tumors (Figure 4G). Thus, BxPC3 MUC1 xenografted tumors exhibited an aggressive phenotype consistent with the human tumors that express high MUC1. This included loss of E-cadherin, induction of Vimentin and upregulation of metastatic and angiogenic factors. It is striking that simply abrogating the signal transduction events by mutating the seven tyrosines can completely reverse the process of EMT and significantly alter the tumor microenvironment, subsequently leading to a less aggressive, less metastatic, and less angiogenic phenotype.

MUC1 interacts with β-catenin and translocates to the nucleus in the BxPC3-MUC1 but not in the Y0 cells

To delineate the underlying mechanism by which the Y0 tumors circumvent EMT, we tested the nuclear localization of MUC1 CT and β-catenin in the MUC1 and Y0 cells. It is known that tyrosine residues in MUC1 CT are critically important for nuclear localization of MUC1 CT and β-catenin (20). Although β-catenin was present in the nuclear extracts in both cells, the levels were significantly higher in BxPC3 MUC1 cells compared to the Y0 cells (Figure 5A). Similar results were obtained with the KCM and KCKO cells where higher levels of β-catenin were detected in the nuclear extract of the KCM versus the KCKO cells (Figure 4B). More importantly, although both BxPC3 MUC1 and Y0 cells contained equal levels of MUC1 (Figure 3A), there was no detectable MUC1 CT in the nuclear extract of the Y0 cells while high levels was detected in the BxPC3 MUC1 cells (Figure 5A). The results were substantiated in Su86.86 MUC1 and Y0 cells (Figure 5C). The data clearly suggests that signaling through the tyrosines is critically important for efficient nuclear translocation of MUC1 CT and β-catenin. Purity of the nuclear extract was confirmed by the presence of lamin and the absence of IKK (Figure 5A–C).

Since tyrosine phosphorylation is required for MUC1 to bind β-catenin and translocate to the nucleus, we examined if β-catenin and MUC1 co-IP in these cells. β-catenin interacted with MUC1 only in the BxPC3-MUC1 cells but minimally in the Y0 cells (Figure 5D). The co-IP of β-catenin and MUC1 was confirmed in the KCM and KCKO cells and in the Su86.86 cells (Figure 5E and F). Thus, we confirm that binding of MUC1 to β-catenin appears to provide the signal required for movement of MUC1 to the nucleus and that the tyrosines in MUC1 CT have to be functional for the two proteins to interact.

Discussion

Although it has been known for decades that MUC1 is aberrantly over-expressed in greater than 95% of metastatic PDA and is associated with poor prognosis, its precise role has remained obscure. We show for the first time in both mouse and human pancreatic tumors that 1) over-expression of MUC1 initiates the process of EMT and augments metastasis and 2) lack of tyrosines in the CT of MUC1 abrogates this process. The first evidence of EMT came from the proteomics data showing repression of E-Cadherin and induction of Vimentin expression in the PDA.MUC1 tumors when compared to the PDA.Muc1KO tumors. This correlated with significantly higher incidence of secondary metastasis in PDA.MUC1 mice as compared to the PDA.Muc1KO mice. The PDA mice are unique in that the pancreatic tumors arise spontaneously in an appropriate tissue background, within a suitable stromal and hormonal milieu, and in the context of a viable immune system (17, 26–27). The tumor progression and the histopathology of the tumors in the PDA mice mimic the human disease with the initial development of pancreatic intra-epithelial neoplastic (PanIN) lesions progressing to carcinoma-in-situ (CIS), and invasive adenocarcinoma. The process of EMT and increased invasiveness in MUC1-expressing pancreatic tumors was confirmed in cell lines generated from the PDA mice and validated in two human pancreatic cell lines. The underlying molecular mechanism in all cell lines pointed to the induction of transcription factors, Snail, and Slug which stimulated the expression of Vimentin and repressed E-Cadherin expression. E-Cadherin plays a key role in the establishment and maintenance of

adherent junctions and loss of the same results in contact inhibition and cell motility. Interestingly, the molecular process of EMT was completely abrogated when all seven tyrosines in the CT of MUC1 were mutated to phenylalanine. Note that the cytoplasmic tail of MUC1 Y0 shows a shift in electrophoretic mobility relative to MUC1 WT; this likely reflects a decrease in phosphorylation due to mutation of the tyrosine residues and therefore change in the overall charge. This has been previously reported in other cell types (28). We do not believe that the change in the electropheretic mobility is due to size since the delta between seven tyrosines and seven phenylalanines is ~67 daltons. Recent evidence shows that the phosphorylation of the tyrosines in the MUC1 CT are critical for the binding of β-catenin to MUC1 CT and that the MUC1 CT-β-catenin complex can be translocated to the nucleus to render its oncogenic signal (29). We show that lack of tyrosines in the MUC1 CT regulates the interaction between MUC1 CT with β-catenin, and therefore its efficient translocation to the nucleus (Figure 5). It is also known that β-catenin binds to the SXXXXXSSL motif in the CT of MUC1 (30) and changes in tyrosine phosphorylation of MUC1 CT correlated with differences in cell adhesion (30–31). Thus, we can speculate that the underlying mechanism for EMT might be the requirement of the tyrosines adjacent to the β-catenin binding domain (possibly at the TDRSPYEKV site) to be phosphorylated. C-src and PKCδ have been shown to phosphorylate the tyrosines at that site and increase the interaction between β-catenin and MUC1 (24, 32). We therefore propose that MUC1 may directly influence the transcriptional co-activator status of β-catenin, and up-regulate several genes that are associated with EMT such as Snail, Slug, Twist, Vimentin and Goosecoid (Figure 2D), possibly through interactions with TCF/LEF1 and/or other transcription factors. Snail in turn represses E-cadherin message and protein levels in MUC1-expressing cells (Figures 1–4), perhaps through direct binding to the three E-boxes in the E-cadherin promoter (6). E-cadherin plays a key role in the establishment and maintenance of adherence junctions, repression of which leads to down regulation of Tight Junction Proteins 1 and 3, Occludin, Laminin α5, and β-and δ-catenins (Figure 2C). Dissolution of pancreatic epithelial cell junctions is hence brought about by a concerted activation of mesenchymal proteins and repression of epithelial proteins *in vitro* and *in vivo* leading to EMT and metastasis exemplified by the presence of CTCs in BxPC3.MUC1 tumors (Figure 4C) and enhanced metastasis in the PDA.MUC1 mice (Figure 1B).

These molecular changes lead to an *in vivo* microenvironment favoring increased angiogenic and pro-inflammatory cytokines in the MUC1 tumors (Figure 4F and G), leading to increased metastasis. The glycoprotein P-selectin, an adhesion molecule involved in the initiation of inflammatory process and induction of IL-6 and its receptors (33–34) was increased by 20 fold in MUC1 versus Neo tumors (Figure 4F). VEGF, a potent inducer of angiogenesis and promoter of tumor progression (35) was increased by 10-fold in the MUC1 tumors (Figure 4F). Lastly, SCF, EGF and IGF-1, factors known to induce growth and proliferation in pancreatic cancer cells (36–37) (38) were increased by 2–3 fold in MUC1 tumors (Figure 4F). Thus, it is indeed striking that the significant induction of these factors in the MUC1 tumors were completely abrogated when the tyrosines in MUC1 CT were deemed non-functional (Figure 4F). This once again signifies the critical requirement of the MUC1 CT tyrosines in pancreatic cancer oncogenesis and metastasis.

The regulation of MUC1 CT phosphorylation and parameters that affect its association with β-catenin are not fully understood, although interaction of MUC1 with ErbB1 (39) has been shown to enhance the binding between c-src, β-catenin and MUC1 (20) and increase ERK1/2 phosphorylation and NFκB activation (28, 39). Preliminary data from our laboratory shows that the active form of NFκB-p65 subunit translocation to the nucleus is negligible in the Y0 cells compared to the MUC1 cells (unpublished data). Our study exemplifies the functional consequences (EMT and metastasis) of signaling through MUC1 CT, and for the first time delineates the role of this protein in a unique mouse model of PDA that lacks Muc1. The data defines the role of MUC1 signaling (through its CT tyrosines) in the initiation of EMT perhaps by β-catenin-MUC1 interaction and translocation to the nucleus, leading to activation of the EMT-associated transcription factors Snail and Slug. This in turn enables the tumors to acquire a highly aggressive phenotype creating a pro-metastatic microenvironment *in vivo*. Future studies will focus on identifying the particular tyrosine/s within MUC1 CT and determining if inhibiting its phosphorylation using small molecule kinase inhibitors may lead to a novel treatment modality for pancreatic cancer.

Materials and Methods

Mouse Model

PDA mice were generated in our laboratory on the C57BL/6 background by mating the P48-Cre with the LSL-KRAS^{G12D} mice (26) and further mated to the MUC1.Tg mice to generate PDA.MUC1 mice (17, 27) or to the Muc1KO mice (15) to generate PDA.Muc1KO mice (Figure 1A). Primary tumors were dissociated using collagenase IV (Worthington Biochemical Corp, NJ) and several lines of cells were generated in our laboratory. These cells are designated KCKO for cells lacking Muc1 and KCM for cells expressing human MUC1.

Invasion Assays

Cells were serum-starved for 24hrs prior to plating for the invasion assay. Cells in serum free media (50,000 cells) were plated over transwell inserts (BD Biosciences) pre-coated with reduced growth factor matrigel, and were permitted to invade towards serum contained in the bottom chamber for 48 hours. Percent invasion was calculated as absorbance of samples/absorbance of controls × 100.

Western Blots and Antibodies

Equal quantities of tumor lysate were loaded on SDS-PAGE gels. MUC1 CT antibody CT2, was made in Mayo Clinic Immunology Core (39). MUC1 TR (B27.29) antibody was acquired from Biomira Inc.,Edmonton, Alberta. All other antibodies (Snail, Slug, N-Cadherin, Vimentin, VEGF, E-Cadherin, β-catenin, and β-actin) were purchased from Santa Cruz Biotechnology, Santa Cruz, CA and were used according to manufacturer's recommendations. Co-immunoprecipitation (co-IP) using CT2 (5μl.) and β-catenin (5μl.) were carried out as previously reported (40) using 1mg of protein lysate prepared in 1% Brij buffer followed by denaturing Western blotting.

Cloning of MUC1 WT and MUC1 Y0 Vectors

MUC1 Y0 was created using the Quick Change mutagenesis kit (Stratagene, La Jolla, CA) (28). Briefly, primers based on the MUC1 sequence were designed containing single-base alterations resulting in mutation of the tyrosine residues (Y) in MUC1 CT to phenylalanine (F) as shown schematically.

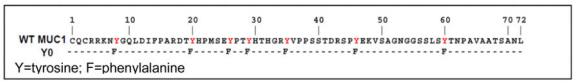

Successful mutations were confirmed with DNA sequencing. MUC1 Y0 and MUC1 WT were cloned into the pLNCX.1 vector consisting of the neomycin resistance gene for retroviral infection. Note: Cells designated as BxPC3.MUC1 or Su89.86. MUC1 represents cells expressing full length MUC1 that consists of the extracellular domain, the transmembrane domain and wild type cytoplasmic tail domain. Cells designated as BxPC3.Y0 or Su89.86. Y0 represents cells expressing full length MUC1 that consists of the extracellular domain, the transmembrane domain and mutant cytoplasmic tail domain in which only the seven tyrosines are replaced by phenylalanine. BxPC3. Neo and Su86.86. Neo represents cells that only express the empty vector and therefore represents the endogenous levels of MUC1in these cells.

Cell Culture and Retroviral Infection

BxPC3 cells and Su86.86 (American Type Culture Collection, Manassas, VA) are two human pancreatic cancer cell lines that express very little endogenous MUC1. For retroviral infection, GP2–293 packaging cells (stably expressing the *gag* and *pol* proteins) were co-transfected with the full-length MUC1 construct or the Y0 construct or empty vector expressing the VSV-G envelope protein as previously described (28). Cells were selected with 0.5 mg/mL G418, beginning 48 hours post infection. Three independent infections of the constructs were carried out with similar results. Expression of the constructs was stable throughout the span of experiments. Cells infected with vector alone were used as control and designated Neo. For MUC1 and Y0-infected cells, MUC1+ve cells were sorted using the FACSAria. For Neo-infected cells, MUC1-ve cells were sorted.

Confocal Microscopy

Cells were plated on chamber slides and grown to the desired confluency. Cells were washed, fixed in –20°C ethanol, permeabilized with 0.5% Tween 20 and stained with E-Cadherin antibody. Nuclei were stained with To-pro-3 (Invitrogen). Pictures were taken at 400X using confocal microscopy (Carl Zeiss International, Thornwood, NY).

Real-time PCR in the Taqman low-density custom made array format

Total RNA was extracted according to standard protocol using the Qiagen RNeasy mini-kit protocol; (Invitrogen, Carson City, CA). cDNA was constructed using TaqMan® Reverse Transcription cDNA kit from Applied Bioscience (Foster City, CA). Each low-density custom array card was configured for 72 different genes in triplicates. The SDS2.2 software was used for qualitative analysis. Arrays were performed independently at least three times

for each cell line; values were obtained for the threshold cycle (Ct) for each gene and normalized using the average of four housekeeping genes on the same array (*HPRT1*, *RPL13A*, *GAPDH*, *ACTB*). Change (ΔCt) between Neo, MUC1, and Y0 was found by: ΔCt = Ct (MUC1 or Y0) – Ct (neo) and fold change by: Fold change = 2(−ΔCt).Values are provided as fold change.

Isolation of Nuclear Protein

Cells were washed in cold PBS and then resuspended in buffer A (10 mM HEPES pH 7.5, 10 mM KCl, 0.1 mM EDTA, 0.1 mM EGTA and 0.1% Nonidet-P40) on ice for 20min. Lysates were spun at 6000 rpm, 1min, 4°C and the resulting pellets were washed twice in PBS before sonication in buffer B (20mM HEPES ph 7.9, 25% glycerol, 400mM NaCl, 1.5mM MgCl2, 0.2mM EDTA, 0.5mM DTT) to obtain the nuclear fraction which was then spun at 13 000 rpm for 20min, 4°C, for Western blot analysis using CT2 and β-catenin antibodies.

In vivo tumor growth

Two-month old nude mice were injected with 5×10^6 tumor cells into the flank of the mice. Tumors were allowed to grow for two months. Mice were palpated every second day starting at 7 days post tumor injection until sacrifice. Tumor weight was calculated according to the following formula: grams=(length in centimeters × $(\text{width})^2$)/2 (41). Upon sacrifice, the tumor portions were prepared for lysates and fixed for immunohistochemistry (IHC).

Immunohistochemistry

Tumor sections were formalin fixed and paraffin embedded blocks were prepared by the Histology Core at The Mayo Clinic and 4-micron thick sections were cut for immunostaining. VEGF expression was determined using the Santa Cruz Biotechnologies antibodies at 1:50 dilution followed by the appropriate secondary antibody (1:100 dilution, DAKO, Carpenteria, CA). Sections were developed using 3, 3”–Diaminobenzidine as the chromogen and hematoxylin as the counterstain. Slides were examined under light microscopy and pictures taken at 400X magnification.

Isolation of viable circulating human pancreatic cancer cells

Blood samples (0.5–1.0 ml) were obtained by cardiac puncture from individual tumor-bearing animals using heparin as the anticoagulant and processed immediately. Erythrocyte-free nucleated cell fractions were obtained using the RBC lysis buffer (Stemcell Technologies, Inc., Vancouver, Canada). This fraction was immediately expanded in culture in DMEM complete media as previously described (42).

Protein Array

Tumor lysates were analyzed using the RayBio® Custom protein array kit (RayBiotech, Norcross, GA). Assay was conducted according to the manufacturer’s instructions (43). Chemiluminescence was detected using a EpiChemi3® Darkroom imaging system and LabWorks® densitometry software (UVP Bioimaging, Upland, CA). Data was corrected for

background signal and normalized to positive controls using RayBio® Analysis Tool software.

Proteomics

For the electrophoretic separation of each sample, 30 ug of protein was loaded on a 10 % Bis-Tris NuPAGE gel (Invitrogen, Carlsbad, CA) and proteomic analysis conducted as previously reported (44). A Nano Acuity UPLC system connected to an LTQ- Orbitrap hybrid MS system (Thermo Fisher, Pittsburg, PA) with Nanospray interface was used. Data was acquired using Xcalibur and searched by Bioworks software (Thermo Fisher, Pittsburg, PA) using IPI mouse v.3.18 fasta database. Search results were entered into Scaffold software (Proteome Software, Portland, OR) for compilation, normalization, and comparison of spectral counts. Datasets were imported into R program for statistical computing.

Statistical analysis

Statistical analysis was performed with SPSS 10 software. P-values were generated using the one way Anova and significance was confirmed using the Duncan and Student-Newman-Keul test. Values were considered significant if $p < 0.05$.

Acknowledgement

We acknowledge the funding provided by NIH CA R01CA118944. We thank Dr. Jennifer Curry for critically reviewing the manuscript. We thank Cathy S. Madison and Carole M. Viso for their technical help with confocal microscopy and cell sorting. We are thankful to for her help with cell sorting. We also acknowledge all the technicians in the animal facility and in the histology core facilities at The Mayo Clinic.

Supported by: funding provided by NIH CA R01CA118944

REFERENCES

1. Chang BW, Siccion E, Saif MW. Updates in locally advanced pancreatic cancer. Highlights from the "2010 ASCO Annual Meeting". Chicago, IL, USA. June 4–8, 2010. JOP. 2010; 11:313–316. [PubMed: 20601800]
2. Burris HA 3rd, Moore MJ, Andersen J, Green MR, Rothenberg ML, Modiano MR, Cripps MC, Portenoy RK, Storniolo AM, Tarassoff P, Nelson R, Dorr FA, Stephens CD, Von Hoff DD. Improvements in survival and clinical benefit with gemcitabine as first-line therapy for patients with advanced pancreas cancer: a randomized trial. J Clin Oncol. 1997; 15:2403–2413. [PubMed: 9196156]
3. Thiery JP. Epithelial-mesenchymal transitions in tumour progression. Nat Rev Cancer. 2002; 2:442–454. [PubMed: 12189386]
4. Nieto MA. The snail superfamily of zinc-finger transcription factors. Nat Rev Mol Cell Biol. 2002; 3:155–166. [PubMed: 11994736]
5. Batlle E, Sancho E, Franci C, Dominguez D, Monfar M, Baulida J, Garcia De Herreros A. The transcription factor snail is a repressor of E-cadherin gene expression in epithelial tumour cells. Nat Cell Biol. 2000; 2:84–89. [PubMed: 10655587]
6. Guaita S, Puig I, Franci C, Garrido M, Dominguez D, Batlle E, Sancho E, Dedhar S, De Herreros AG, Baulida J. Snail induction of epithelial to mesenchymal transition in tumor cells is accompanied by MUC1 repression and ZEB1 expression. J Biol Chem. 2002; 277:39209–39216. [PubMed: 12161443]
7. Cano A, Perez-Moreno MA, Rodrigo I, Locascio A, Blanco MJ, del Barrio MG, Portillo F, Nieto MA. The transcription factor snail controls epithelial-mesenchymal transitions by repressing E-cadherin expression. Nat Cell Biol. 2000; 2:76–83. [PubMed: 10655586]

8. Comijn J, Berx G, Vermassen P, Verschueren K, van Grunsven L, Bruyneel E, Mareel M, Huylebroeck D, van Roy F. The two-handed E box binding zinc finger protein SIP1 downregulates E-cadherin and induces invasion. Mol Cell. 2001; 7:1267–1278. [PubMed: 11430829]
9. Bolos V, Peinado H, Perez-Moreno MA, Fraga MF, Esteller M, Cano A. The transcription factor Slug represses E-cadherin expression and induces epithelial to mesenchymal transitions: a comparison with Snail and E47 repressors. J Cell Sci. 2003; 116:499–511. [PubMed: 12508111]
10. Fujita N, Jaye DL, Kajita M, Geigerman C, Moreno CS, Wade PA. MTA3, a Mi-2/NuRD complex subunit, regulates an invasive growth pathway in breast cancer. Cell. 2003; 113:207–219. [PubMed: 12705869]
11. Peinado H, Quintanilla M, Cano A. Transforming growth factor beta-1 induces snail transcription factor in epithelial cell lines: mechanisms for epithelial mesenchymal transitions. J Biol Chem. 2003; 278:21113–21123. [PubMed: 12665527]
12. Zhou BP, Deng J, Xia W, Xu J, Li YM, Gunduz M, Hung MC. Dual regulation of Snail by GSK-3beta-mediated phosphorylation in control of epithelial-mesenchymal transition. Nat Cell Biol. 2004; 6:931–940. [PubMed: 15448698]
13. Lan MS, Batra SK, Qi WN, Metzgar RS, Hollingsworth MA. Cloning and sequencing of a human pancreatic tumor mucin cDNA. J Biol Chem. 1990; 265:15294–15299. [PubMed: 2394722]
14. Patton S, Gendler SJ, Spicer AP. The epithelial mucin, MUC1, of milk, mammary gland and other tissues. Biochim Biophys Acta. 1995; 1241:407–423. [PubMed: 8547303]
15. Spicer AP, Rowse GJ, Lidner TK, Gendler SJ. Delayed mammary tumor progression in Muc-1 null mice. J Biol Chem. 1995; 270:30093–30101. [PubMed: 8530414]
16. Schroeder JA, Adriance MC, Thompson MC, Camenisch TD, Gendler SJ. MUC1 alters beta-catenin-dependent tumor formation and promotes cellular invasion. Oncogene. 2003; 22:1324–1332. [PubMed: 12618757]
17. Tinder TL, Subramani DB, Basu GD, Bradley JM, Schettini J, Million A, Skaar T, Mukherjee P. MUC1 enhances tumor progression and contributes toward immunosuppression in a mouse model of spontaneous pancreatic adenocarcinoma. J Immunol. 2008; 181:3116–3125. [PubMed: 18713982]
18. Carson DD. The cytoplasmic tail of MUC1: a very busy place. Sci Signal. 2008; 1:pe35. [PubMed: 18612140]
19. Singh PK, Hollingsworth MA. Cell surface-associated mucins in signal transduction. Trends Cell Biol. 2006; 16:467–476. [PubMed: 16904320]
20. Hollingsworth MA, Swanson BJ. Mucins in cancer: protection and control of the cell surface. Nat Rev Cancer. 2004; 4:45–60. [PubMed: 14681689]
21. Mukherjee P, Tinder TL, Basu GD, Gendler SJ. MUC1 (CD227) interacts with lck tyrosine kinase in Jurkat lymphoma cells and normal T cells. J Leukoc Biol. 2005; 77:90–99. [PubMed: 15513966]
22. Hattrup CL, Gendler SJ. Structure and function of the cell surface (tethered) mucins. Annu Rev Physiol. 2008; 70:431–457. [PubMed: 17850209]
23. Kufe DW. Targeting the human MUC1 oncoprotein: a tale of two proteins. Cancer Biol Ther. 2008; 7:81–84. [PubMed: 18347419]
24. Ren J, Li Y, Kufe D. Protein kinase C delta regulates function of the DF3/MUC1 carcinoma antigen in beta-catenin signaling. J Biol Chem. 2002; 277:17616–17622. [PubMed: 11877440]
25. Ren J, Bharti A, Raina D, Chen W, Ahmad R, Kufe D. MUC1 oncoprotein is targeted to mitochondria by heregulin-induced activation of c-Src and the molecular chaperone HSP90. Oncogene. 2006; 25:20–31. [PubMed: 16158055]
26. Hingorani SR, Petricoin IIIEF, Maitra A, Rajapaske V, King C, Jacobetz MA, Ross S, Conrads TP, Veenstra TD, Hitt BA, Kawaguchi Y, Johann D, Liotta LA, Crawford HC, Putt MA, Jacks T, Wright CV, Hruban R, Lowy AM, Tuveson DA. Preinvasive and invasive ductal pancreatic cancer and its early detection in the mouse. Cancer Cell. 2003; 4:437–450. [PubMed: 14706336]
27. Mukherjee P, Basu GD, Tinder TL, Subramani DB, Bradley JM, Arefayene M, Skaar T, De Petris G. Progression of pancreatic adenocarcinoma is significantly impeded with a combination of vaccine and COX-2 inhibition. J Immunol. 2009; 182:216–224. [PubMed: 19109152]

28. Thompson EJ, Shanmugam K, Hattrup CL, Kotlarczyk KL, Gutierrez A, Bradley JM, Mukherjee P, Gendler SJ. Tyrosines in the MUC1 cytoplasmic tail modulate transcription via the extracellular signal-regulated kinase 1/2 and nuclear factor-kappaB pathways. Mol Cancer Res. 2006; 4:489–497. [PubMed: 16849524]

29. Wen Y, Caffrey TC, Wheelock MJ, Johnson KR, Hollingsworth MA. Nuclear association of the cytoplasmic tail of MUC1 and beta-catenin. J Biol Chem. 2003; 278:38029–38039. [PubMed: 12832415]

30. Yamamoto M, Bharti A, Li Y, Kufe D. Interaction of the DF3/MUC1 breast carcinoma-associated antigen and beta-catenin in cell adhesion. J Biol Chem. 1997; 272:12492–12494. [PubMed: 9139698]

31. Quin RJ, McGuckin MA. Phosphorylation of the cytoplasmic domain of the MUC1 mucin correlates with changes in cell-cell adhesion. Int J Cancer. 2000; 87:499–506. [PubMed: 10918188]

32. Li Y, Kufe D. The Human DF3/MUC1 carcinoma-associated antigen signals nuclear localization of the catenin p120(ctn). Biochem Biophys Res Commun. 2001; 281:440–443. [PubMed: 11181067]

33. Kaikita K, Ogawa H, Yasue H, Sakamoto T, Suefuji H, Sumida H, Okumura K. Soluble P-selectin is released into the coronary circulation after coronary spasm. Circulation. 1995; 92:1726–1730. [PubMed: 7545553]

34. Dymicka-Piekarska V, Matowicka-Karna J, Gryko M, Kemona-Chetnik I, Kemona H. Relationship between soluble P-selectin and inflammatory factors (interleukin-6 and C-reactive protein) in colorectal cancer. Thromb Res. 2007; 120:585–590. [PubMed: 17169411]

35. Justinger C, Schluter C, Oliviera-Frick V, Kopp B, Rubie C, Schilling MK. Increased growth factor expression after hepatic and pancreatic resection. Oncol Rep. 2008; 20:1527–1531. [PubMed: 19020737]

36. Mroczko B, Szmitkowski M, Wereszczynska-Siemiatkowska U, Jurkowska G. Hematopoietic cytokines in the sera of patients with pancreatic cancer. Clin Chem Lab Med. 2005; 43:146–150. [PubMed: 15843207]

37. Bardeesy N, DePinho RA. Pancreatic cancer biology and genetics. Nat Rev Cancer. 2002; 2:897–909. [PubMed: 12459728]

38. Wolpin BM, Michaud DS, Giovannucci EL, Schernhammer ES, Stampfer MJ, Manson JE, Cochrane BB, Rohan TE, Ma J, Pollak MN, Fuchs CS. Circulating insulin-like growth factor axis and the risk of pancreatic cancer in four prospective cohorts. Br J Cancer. 2007; 97:98–104. [PubMed: 17533398]

39. Schroeder JA, Thompson MC, Gardner MM, Gendler SJ. Transgenic MUC1 interacts with EGFR and correlates with MAP kinase activation in the mouse mammary gland. J. Biol. Chem. 2001; 276:13057–13064. [PubMed: 11278868]

40. Al Masri A, Gendler SJ. Muc1 affects c-Src signaling in PyV MT-induced mammary tumorigenesis. Oncogene. 2005; 24:5799–5808. [PubMed: 15897873]

41. Simpson-Herren L, Lloyd HH. Kinetic parameters and growth curves for experimental tumor systems. Cancer Chemother Rep. 1970; 54:143–174. [PubMed: 5527016]

42. Glinskii AB, Smith BA, Jiang P, Li XM, Yang M, Hoffman RM, Glinsky GV. Viable circulating metastatic cells produced in orthotopic but not ectopic prostate cancer models. Cancer Res. 2003; 63:4239–4243. [PubMed: 12874032]

43. Das Roy L, Pathangey LB, Tinder TL, Schettini JL, Gruber HE, Mukherjee P. Breast cancer-associated metastasis is significantly increased in a model of autoimmune arthritis. Breast Cancer Res. 2009; 11:R56. [PubMed: 19643025]

44. Hwang SI, Lundgren DH, Mayya V, Rezaul K, Cowan AE, Eng JK, Han DK. Systematic characterization of nuclear proteome during apoptosis: a quantitative proteomic study by differential extraction and stable isotope labeling. Mol Cell Proteomics. 2006; 5:1131–1145. [PubMed: 16540461]

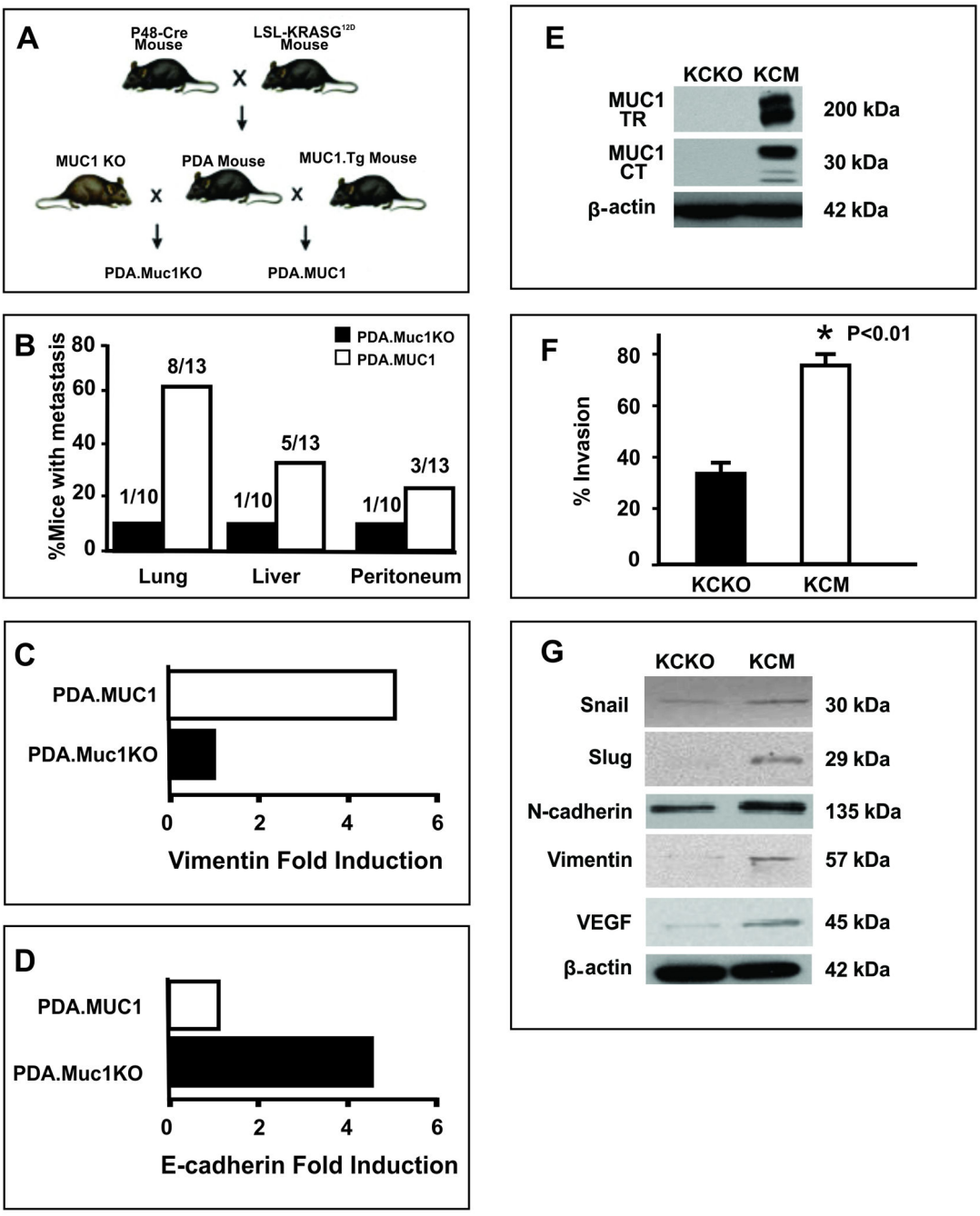

Figure 1. PDA mice lacking Muc1 have significantly lower incidence of secondary metastasis associated with decreased induction of EMT proteins in the tumors

A. Schematic representation of PDA, PDA.MUC1 and PDA.Muc1KO mice. PDA mice were mated to the human MUC1.Tg and mouse Muc1 KO mice to get PDA.MUC1 mice and PDA.MUC1 KO mice respectively. **B**. Percent mice that developed metastasis in PDA.MUC1 versus PDA.MUC1 KO mice. **C and D**. Proteomics data on PDA.MUC1 and PDA.Muc1 KO tumor lysates showing E-cadherin repression and Vimentin upregulation. **E**. Western blot analysis of MUC1 expression for KCM and KCKO cells using MUC1 TR and

MUC1 CT monoclonal antibodies. **F**. Transwell invasion assay showing significantly higher invasion index for KCM cells compared to KCKO cells (*P<0.001). **G**. Gain of mesenchymal proteins in KCM cells versus KCKO cells. β-actin serves as control for equal protein loading.

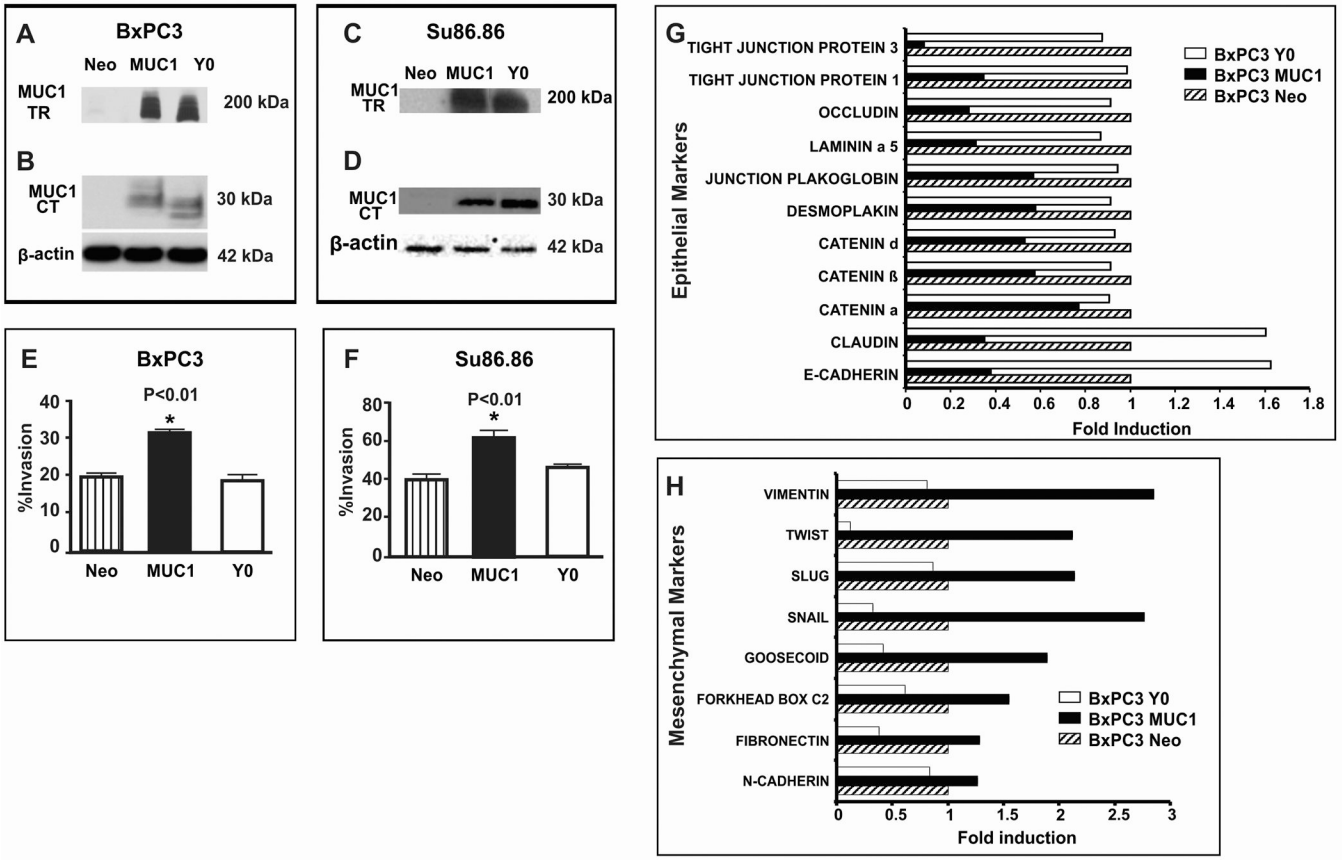

Figure 2. Significantly higher invasion and transcription of genes associated with a mesenchymal phenotype coupled with significantly lower transcription of genes associated with an epithelial phenotype in MUC1 over-expressing human pancreatic cancer cells as compared to control cells. Complete reversal in the MUC1.Y0 expressing cells

MUC1 expression by Western blot analysis: **A**. MUC1 TR and **B**. MUC1 CT expression of BxPC3 Neo, MUC1, and Y0; **C**. MUC1 TR and **D**. MUC1 CT staining of Su86.86 Neo, MUC1, and Y0. >200kDa represents MUC1 TR domain and 30kD represents MUC1 CT domain. β-actin was used as loading control. **E - F**. *In vitro* trans-well invasion assay for BxPC3 and Su86.86 cells respectively; Compared to Neo and Y0 cells, MUC1-expressing cells have significantly higher invasion index (* p<0.001). **G - H**. RT-PCR analysis of BxPC3 Neo, MUC1, and Y0 cells: **G**. Transcription of genes generally associated with epithelial phenotype. **H**. Transcription of genes generally associated with mesenchymal phenotype. Genes whose transcription was altered by at least 2-fold or more were considered significant. Average fold change is shown from three separate experiments. All experiments were repeated 3 times with a R-value (Correlation Coefficient) of >0.98. Clones from three independent infections were analyzed with similar results.

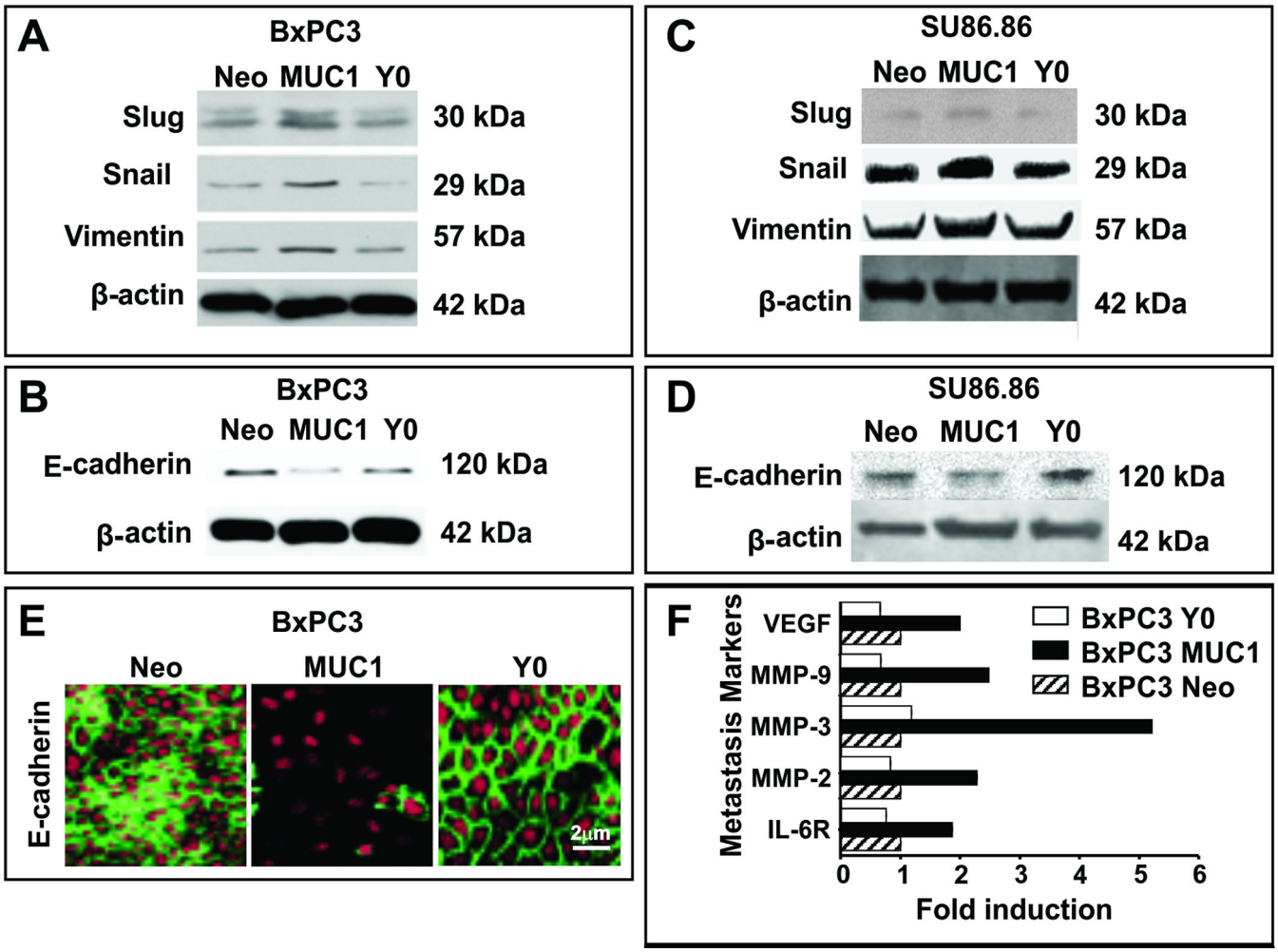

Figure 3. Repression of E-Cadherin and induction of Snail, Slug, and Vimentin in MUC1 cells coupled with significantly increased transcription of genes associated with metastasis. Complete reversal in MUC1-Y0 expressing cells

A – D. Western blotting analysis of Slug, Snail, Vimentin **(A and C)**, and E-Cadherin (**B and D**) expression in BxPC3 and Su86.86 respectively. Neo, MUC1, and Y0 cells are shown. **E**. Immunofluorescence staining and confocal microscopic image of E-Cadherin levels in BxPC3 Neo, MUC1 and Y0 cells. Images were taken at 400X magnification. The experiments were repeated 3 times with three separate clones with similar results. β-actin was used as loading control. **F**. RT-PCR analysis of genes generally associated with metastasis and angiogenesis. 2-fold or more difference was considered significant. Average fold change is shown from three separate experiments.

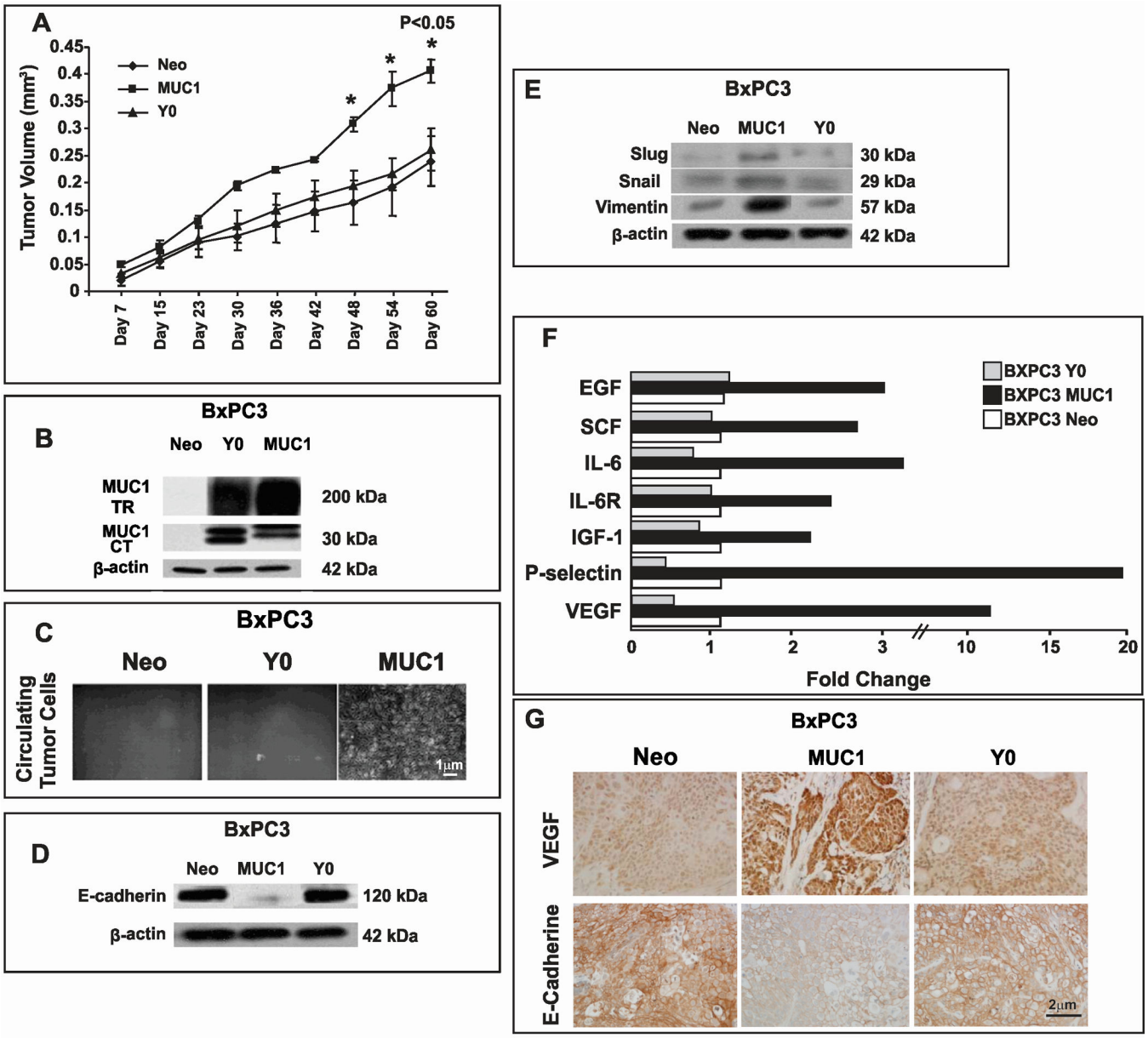

Figure 4. Higher tumor burden with loss of E-Cadherin and gain of mesenchymal and metastatic proteins in BxPC3 MUC1 versus Y0 and Neo tumors

A. *In vivo* tumor growth in nude mice. Significantly higher tumor burden in BxPC3. MUC1 versus Neo and Y0 tumors (*$p < 0.001$). **B**. MUC1 expression by Western blotting using the MUC1 TR and CT antibodies **C**. Tumor cells cultured from whole blood of tumor-bearing mice. Circulating tumor cells detected in the blood of mice bearing the BxPC3 MUC1 but not BxPC3 Y0 or Neo tumors. **D**. *E*xpression of E-Cadherin in primary tumors by Western blotting. **E**. *E*xpression of Slug, Snail, and Vimentin in primary tumors by Western blotting. **F**. High levels of pro-metastatic and pro-angiogenic proteins detected in the BXPC3 MUC1 tumor lysate. Fold change in levels of various factors in BxPC3 MUC1 tumor lysate compared to Y0 and Neo, **G**. Expression of VEGF and E-cadherin by IHC. Images were taken at 400X magnification. Similar results with n=3 mice were obtained.

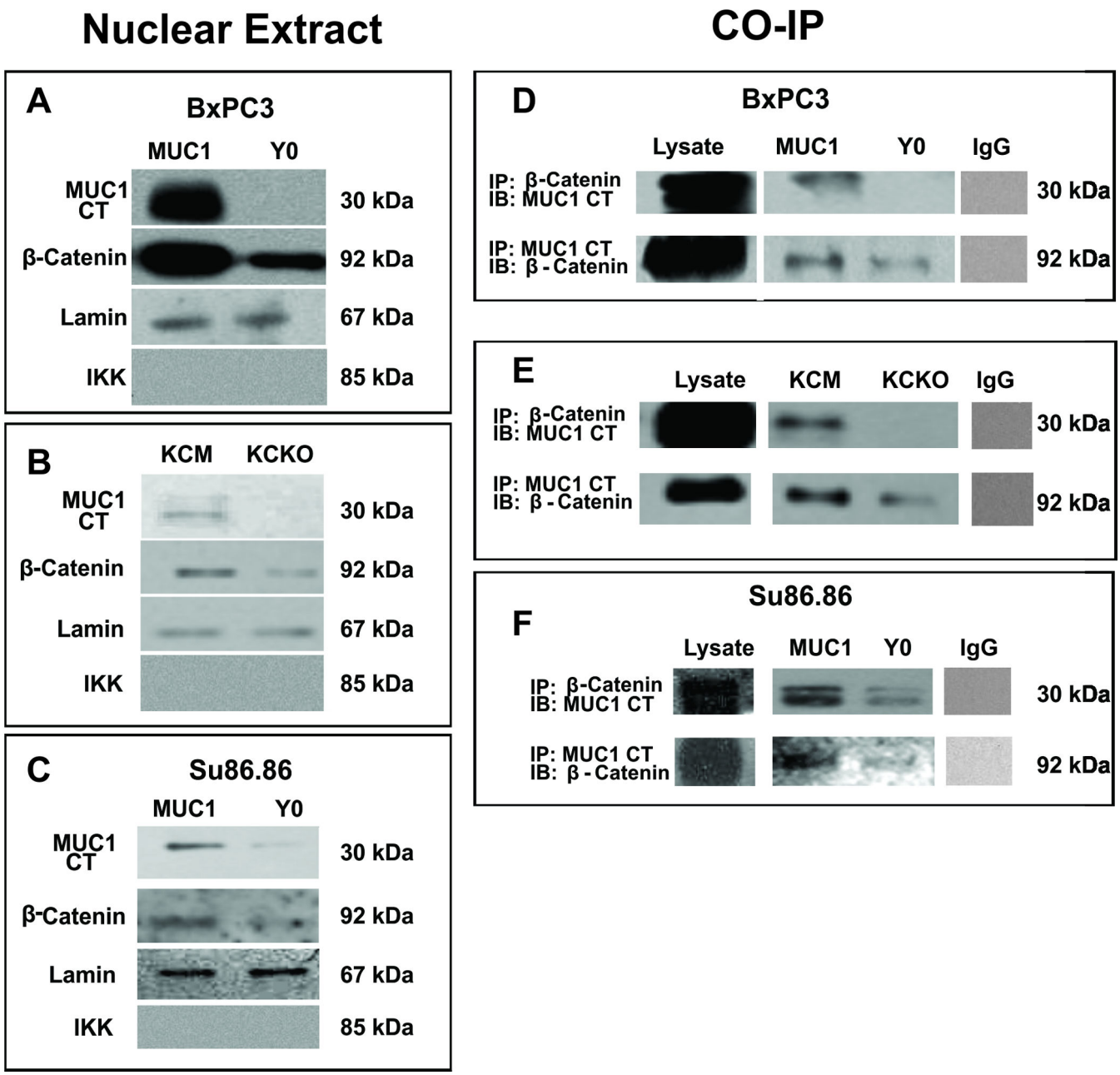

Figure 5. MUC1 interacts with β-catenin and translocates to the nucleus in the MUC1-expressing cells. Complete reversal in the Y0 cells

Protein expression of MUC1 CT and β-catenin in the nuclear extracts of **A**. BxPC3 MUC1 and Y0; **B**. KCM and KCKO and **C**. Su86.86 MUC1 and Y0 cells. Lamin and IKK used as positive and negative control for nuclear extracts. Co-IP of MUC1 CT and β-catenin in both directions from **D**. BxPC3 MUC1 and Y0; **E**. KCM and KCKO and **F**. Su86.86 MUC1 and Y0 cells. Non-specific pull down was not detected using an IgG control antibody. *Note: Neo cells were not included in the data as they express minimal levels of endogenous MUC1 and we found little to no β-catenin or MUC1 CT in the nucleus (data not shown)*